Biochemical and Biophysical Research Communications 428 (2012) 427–432

Contents lists available at SciVerse ScienceDirect

Biochemical and Biophysical Research Communications

journal homepage: www.elsevier.com/locate/ybbrc

# Crystal structure of the *Candida albicans* Kar3 kinesin motor domain fused to maltose-binding protein

Caroline Delorme, Monika Joshi, John S. Allingham *

*Department of Biomedical and Molecular Sciences, Queen's University, Kingston, ON, Canada K7L 3N6*

ARTICLE INFO

*Article history:*
Received 30 September 2012
Available online 5 November 2012

*Keywords:*
*Candida albicans*
Kinesin
Kar3
Maltose-binding protein
Crystal structure

ABSTRACT

In the human fungal pathogen *Candida albicans*, the Kinesin-14 motor protein Kar3 (*Ca*Kar3) is critical for normal mitotic division, nuclear fusion during mating, and morphogenic transition from the commensal yeast form to the virulent hyphal form. As a first step towards detailed characterization of this motor of potential medical significance, we have crystallized and determined the X-ray structure of the motor domain of *Ca*Kar3 as a maltose-binding protein (MBP) fusion. The structure shows strong conservation of overall motor domain topology to other Kar3 kinesins, but with some prominent differences in one of the motifs that compose the nucleotide-binding pocket and the surface charge distribution. The MBP and Kar3 modules are arranged such that MBP interacts with the Kar3 motor domain core at the same site where the neck linker of conventional kinesins docks during the "ATP state" of the mechanochemical cycle. This site differs from the Kar3 neck–core interface in the recent structure of the *Sc*Kar3-Vik1 heterodimer. The position of MBP is also completely distinct from the Vik1 subunit in this complex. This may suggest that the site of MBP interaction on the *Ca*Kar3 motor domain provides an interface for the neck, or perhaps a partner subunit, at an intermediate state of its motile cycle that has not yet been observed for Kinesin-14 motors.



## 1. Introduction

Kinesin motor proteins transport intracellular cargos along microtubules (MTs) and influence the organization and dynamics of the microtubule (MT) cytoskeleton. They are typically composed of 4 domains; a motor domain, a neck or neck-linker, an α-helical coiled-coil forming region, and a cargo binding domain [1]. Of these domains, the motor domain is the most highly conserved (~40% shared identity) and is the key element that binds and hydrolyses ATP as part of the mechanochemical cycle responsible for kinesin movement [2,3]. During this cycle, conserved elements of the motor domain couple ATP binding, hydrolysis, and product release to conformational changes in the motor domain core that regulate MT affinity and guide re-orientation of the neck or neck-linker to produce direction-biased displacement of the kinesin and its cargo.

The kinesin superfamily is comprised of 14 different subfamilies, which are differentiated based on sequence, structure, function, and their directionality along MTs [1,4]. The main role of some kinesin families is to mediate proper cell division through their involvement in mitotic spindle assembly and stabilization, as well as chromosome movement [5]. The Kar3 kinesin from the *Saccharomyces cerevisiae* is a well-studied mitotic kinesin, and is designated a member of the Kinesin-14 family due to its C-terminal motor domain and minus-end-directed movement on MTs [6–8]. Like several other members of the Kinesin-14 family, Kar3 has a second MT-binding site located in the cargo binding domain, allowing it to cross-link and slide MTs of opposite polarity past each other via a power-stroke motility mechanism [7,9,10]. This functionality allows it to mediate mitotic spindle organization by generating inward forces that pull the spindles toward the mid-zone and bundle the MTs [11,12]. *S. cerevisiae* Kar3 is unique from most other kinesin isoforms because it interacts with two distinct kinesin-associated proteins (KAPs), named Cik1 and Vik1, which both lack the capacity to bind and hydrolyze ATP and yet can bind MTs and differentially influence the spatial and temporal localization of Kar3 [9,11,13,14]. Moreover, the *Sc*Kar3Cik1 and *Sc*Kar3Vik1 complexes play discrete and important roles during mitotic division, meiosis, and karyogamy [9,11,15–17].

Recent studies have shown that deleting the KAR3 gene in the related diploid ascomycete fungus *C. albicans* interfered with nor-

*Abbreviations: E. coli*, *Escherichia coli*; MD, motor domain; MT, microtubule; MTs, microtubules; MBP, maltose-binding protein; *Sc*, *Saccharomyces cerevisiae*; *Ca*, *Candida albicans*; KAPs, kinesin-associated proteins; MAPs, microtubule-associated proteins; MTT, maltotetrose.

* Corresponding author. Address: Department of Biomedical and Molecular Sciences, Queen's University, 18 Stuart St., Rm 652, Kingston, ON, Canada K7L 3N6. Fax: +1 613 533 2022.

*E-mail address:* allinghj@queensu.ca (J.S. Allingham).

0006-291X/$ - see front matter © 2012 Elsevier Inc. All rights reserved.
http://dx.doi.org/10.1016/j.bbrc.2012.10.101

**Table 1**
Data collection and refinement statistics.

| | MBP–CaKar3MD |
|---|---|
| Space group | $P2_1$ |
| Cell dimensions | |
| a, b, c (Å) | 49.46, 74.93, 98.67 |
| α, β, γ (°) | 90.00, 96.44, 90.00 |
| Resolution (Å)[a] | 20–2.15 (2.5–2.15) |
| $R_{merge}$[a] | 8.1 (33.7) |
| $I/I$[a] | 12.02 (3.83) |
| Completeness (%)[a] | 98.8 (99.4) |
| Redundancy[a] | 3.16 (3.15) |
| No. observed reflections | 122,186 |
| No. reflections used | 36,680 |
| $R_{work}/R_{free}$[b] | 16.9/21.1 |
| No. atoms | |
| Protein | 5105 |
| MgADP | 28 |
| MTT | 45 |
| Water | 390 |
| Average B-factors (Å$^2$) | |
| Protein | 30.46 |
| MgADP | 38.47 |
| MTT | 31.09 |
| Water | 33.6 |
| R.m.s deviations | |
| Bond lengths (Å) | 0.005 |
| Bond angles (°) | 0.932 |
| Favored | 92.0 |
| Allowed | 7.3 |
| Generously Allowed | 0.7 |
| Outliers | 0.0 |

[a] Data in parentheses represent highest resolution shell.
[b] $R_{factor} = \Sigma||F_{(obs)} - F_{(calc)}||/\Sigma|F_{(obs)}|$, where $R_{work}$ refers to the $R_{factor}$ for the data utilized in the refinement and $R_{free}$ refers to the $R_{factor}$ for 5% of the data that were excluded from the refinement.

mal morphogenesis of mating projections and abrogated nuclear fusion during karyogamy [18]. KAR3 knockout strains also exhibited longer generation times and lower cell viability of mitotically dividing yeast, suggesting that the Kar3 kinesin protein plays an important role in mitosis and mating of *C. albicans*. Given that this commensal fungus can cause debilitating mucosal infections, as well as life-threatening systemic infections [19,20] in times of stress or in immune-compromised individuals, these insights highlight the potential for use of the *C. albicans* Kar3 kinesin as a novel target for antifungal drugs.

To begin building a molecular description of *C. albicans* Kar3, we have solved the X-ray crystal structure of its motor domain as a C-terminal fusion with maltose-binding protein (MBP). This is the first *C. albicans* motor protein structure to be determined and although its overall structure shows considerable homology with previously obtained structures of Kar3 from *S. cerevisiae* [10,21,22], and the filamentous fungus *Ashbya gossypii* [23], a number of unique features of the motor domain are apparent. Also, the close spatial arrangement of the MBP and *Ca*Kar3 motor domain (*Ca*Kar3MD) modules indicates the existence of an interface on *Ca*-Kar3 that may be involved in intramolecular or intermolecular interactions that are new to the Kinesin-14 family.

## 2. Materials and methods

### 2.1. Cloning, protein expression, and purification

cDNA for full-length *Ca*Kar3 was amplified from genomic DNA (ATCC number: 10231D-5), inserted into the TOPO cloning vector (Invitrogen), and sequenced to verify its identity. The *Ca*Kar3MD construct (Leu344–Lys687) was amplified by PCR and cloned into pET14d (Novagen) using NcoI and NotI restriction sites for untagged protein expression, or into pMal-MATa1 (Addgene) using HindIII and PstI for expression as a maltose-binding protein fusion [24]. Both vectors were expressed in the BL21-CodonPlus (DE3)-RIL *E. coli* cell line (Stratagene) in Luria–Bertani (LB) media supplemented with the appropriate antibiotics as previously described [23]. The untagged *Ca*Kar3MD construct was purified by ion-exchange chromatography (DEAE SP Sepharose Fast Flow, GE Healthcare) as described previously [25]. For the MBP–*Ca*Kar3MD construct, cells were re-suspended in Column Buffer (10 mM $NaPO_4$ pH 7.2, 200 mM NaCl, 2 mM $MgCl_2$, 1 mM EGTA, 1 mM DTT, 0.2 mM ATP, 5 mM β-mercaptoethanol and EDTA-free protease inhibitors (Sigma–Aldrich) and lysed on ice by sonication. Soluble protein was recovered by centrifugation at 21,000 rpm for 30 min in a Beckman JA-25.5 rotor, and the supernatant was loaded onto an amylose resin column (New England Biolabs) that had been equilibrated with Column Buffer. After thorough washing with Column Buffer, MBP–*Ca*Kar3MD was eluted with Column Buffer supplemented with 10 mM maltose. Peak fractions containing purified MBP–*Ca*Kar3MD were pooled and further purified by size exclusion chromatography in 20 mM Hepes, pH 7.2, 1 mM $MgCl_2$, 150 mM NaCl, 1 mM DTT, 0.1 mM ATP. For both protein constructs, final peak fractions were pooled and concentrated with Amicon Ultra concentrators (Millipore) and flash frozen in liquid nitrogen for storage at −80 °C.

### 2.2. Crystallization, data collection and processing, and structure determination

Crystals of the MBP–*Ca*Kar3MD fusion grew by hanging-drop vapor-diffusion at 4 °C after mixing protein (29 mg/ml) supplemented with 2 mM Mg-ATP in a 1:1 volume ratio with a solution of 0.1 M Hepes pH 7.5, 14% PEG 4000, 75 mM NaCl and 5% ethylene glycol. Plate-like crystals appeared after approximately 30 days and were flash-frozen in cyoprotectant comprised of the precipitant solution supplemented with 25% ethylene glycol. X-ray diffraction data were collected from a single frozen crystal on the GM/CA-CAT beam line; station 23 ID/B, at the Argonne National Laboratory (Argonne, IL), and were integrated and scaled with the program XDS [26]. The structure of MBP–*Ca*Kar3MD was solved by molecular replacement using coordinates for *Sc*Kar3MD (PDB: 3KAR) [21] and MBP (PDB: 1MH3) [24] as search models using AutoMR [27]. A series of manual building cycles using *Coot* [28,29] and iterative restrained refinement cycles using *Phenix_Refine* [30] were performed to generate the final model. Data collection and refinement statistics are summarized in Table 1. Coordinates and structure factors have been deposited in the Protein Data Bank with accession number 4H1G.

### 2.3. Microtubule-binding assay

The affinity of *Ca*Kar3MD and MBP–*Ca*Kar3MD for microtubules was determined as described previously [31], with the following modifications. Reactions of 100 µl microtubules (0–6 µM) were incubated with 4 µM kinesin and 2 mM MgAMPPNP for 15 min at room temperature in ATPase Buffer (20 mM HEPES, 5 mM magnesium acetate, 0.1 mM EGTA, 0.1 mM EDTA, 25 mM potassium acetate, 1 mM DTT, 40 µM Taxol, pH 7.2). Reaction mixtures were sedimented by centrifugation at 312,530×*g* in a TLA100 rotor for 15 min at 25 °C. Supernatant and pellet fractions were analyzed by SDS–PAGE and visualized with Coomassie Brilliant Blue R-250.

## 3. Results and discussion

### 3.1. Overall structure of the CaKar3 motor domain

To date, numerous kinesin motor domain structures, as well as structures of multi-subunit kinesin motor complexes, have been

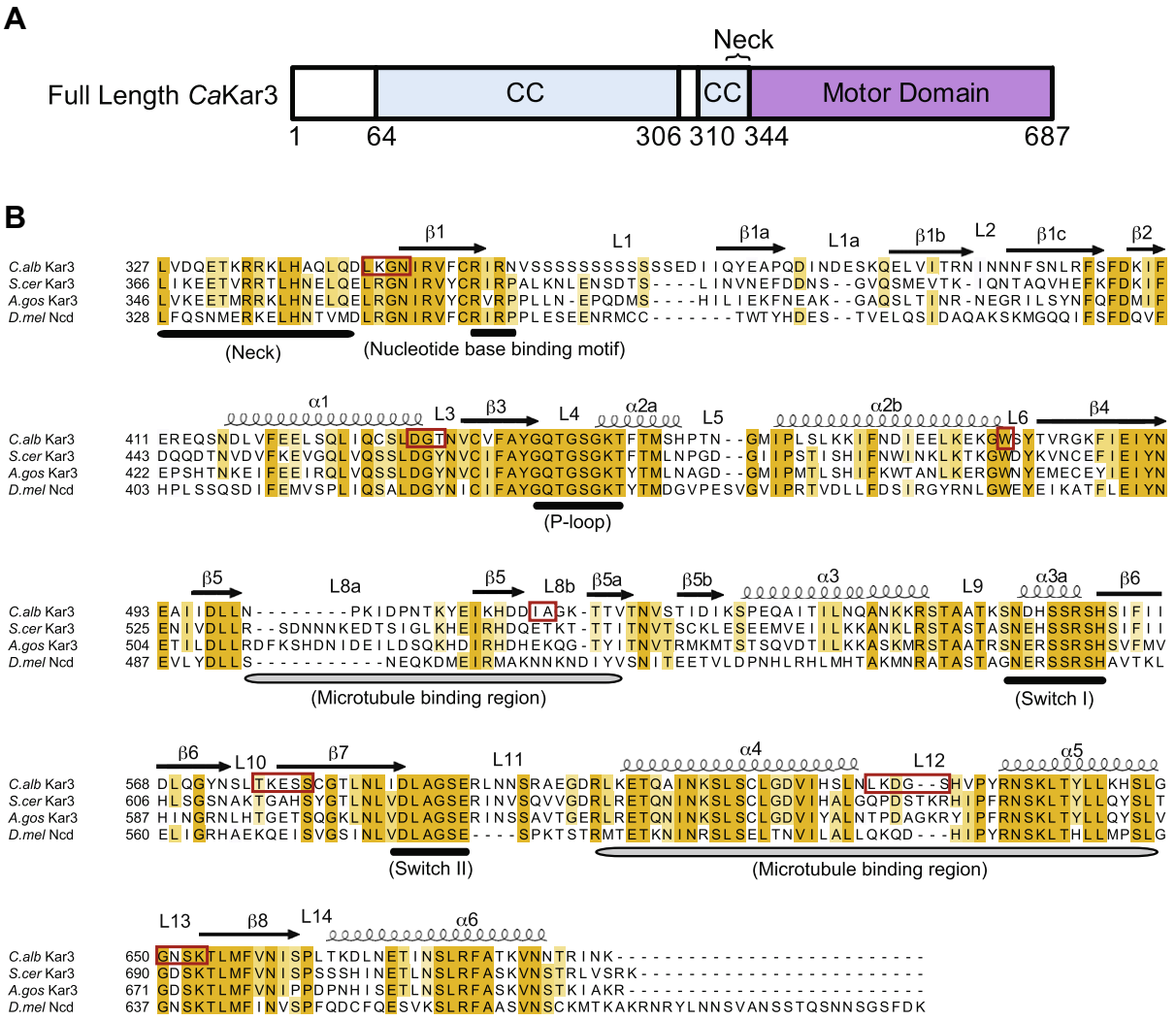


**Fig. 1.** Primary structure of *Ca*Kar3 and sequence alignment of the motor domains of Kar3-related kinesins. (A) Domain organization of *Ca*Kar3 showing coiled-coil forming regions (CC), the neck, and the motor domain location. (B) Alignment of Kinesin-14 motor domains was performed using Clustal W [46]. Intensity of the orange shading is correlated to the degree of shared sequence identity and was created using Jalview [47]. Secondary structure elements were assigned by ESPript according to the *Sc*Kar3MD crystal structure (PDB: 3KAR). Positions of the the nucleotide-binding pocket and MT-binding elements are indicated. Regions boxed in red form non-symmetry contacts with MBP. (For interpretation of the references to color in this figure legend, the reader is referred to the web version of this article.)

deposited in the PDB for a number of different organisms. Some of these include Kinesin-14 motors, such as *Drosophila* Ncd and Kar3 from *S. cerevisiae* [10,21,22,32]. *Ca*Kar3 is 687 amino acids long and its motor domain resides between Leu344 and Lys687 (Fig. 1A) [33]. Sequence conservation between *Ca*Kar3 and other Kinesin-14 family members breaks down significantly at areas that form the small β1-lobe (β1a, β1b, and β1c) at the edge of the motor domain and at the microtubule-binding cluster (L8a, β5a, L8b, and β5b) (Fig. 1B). The region beyond the neck at the N-terminus of the motor domain shares much lower sequence identity with these kinesins, which is typical of all kinesin motors (not shown). To begin to better understand the structural nature of *Ca*Kar3, we pursued structural studies of its motor domain using X-ray crystallography. Although recombinantly expressed *Ca*Kar3MD could be obtained in low, but suitable quantities of acceptable purity, it failed to crystallize even after extensive precipitant screening. However, by fusing maltose-binding protein (MBP) to the N-terminus of the *Ca*Kar3MD via a short polyalanine linker (Fig. 2A), we were able to crystallize and determine the structure of this engineered chimera (MBP–*Ca*Kar3MD) to 2.15 Å.

The MBP and *Ca*Kar3MD components each form a distinct domain within the structure, and electron density for the short polyalanine linker between the two was suitable for modeling this sequence (Fig. 2B). *Ca*Kar3MD adopts the canonical α/β kinesin motor domain fold involving an eight-stranded β-sheet core sandwiched by three exposed α-helices on either side [34]. The final electron density map allowed complete building of residues Leu344–Val357, Asp371–Gln379, Gln387–Lys546, His557–Arg594, Arg604–Asn682 of *Ca*Kar3, and showed MgADP within the nucleotide-binding pocket. The main areas of disorder were confined mainly to surface loops, which is a characteristic feature of most classes of kinesin. The structure of MBP, on the other hand, could be modeled in its entirety and showed maltotetrose (MTT) in its binding pocket. Interactions between symmetric units in the crystal lattice appear to be shared equally between the MBP and *Ca*Kar3MD modules.

### 3.2. Comparison to homologous kinesins

*Ca*Kar3MD shares high tertiary structure similarity with the *A. gossypii* Kar3 motor domain (PDB code 3T0Q) [23] and the *Sc*Kar3 motor domain from the recently determined *Sc*Kar3Vik1 heterodimer (PDB code 4ETP) [10], where their RMS deviations for 257 and 271 structurally equivalent α-carbons are 0.699 Å and 0.802 Å,

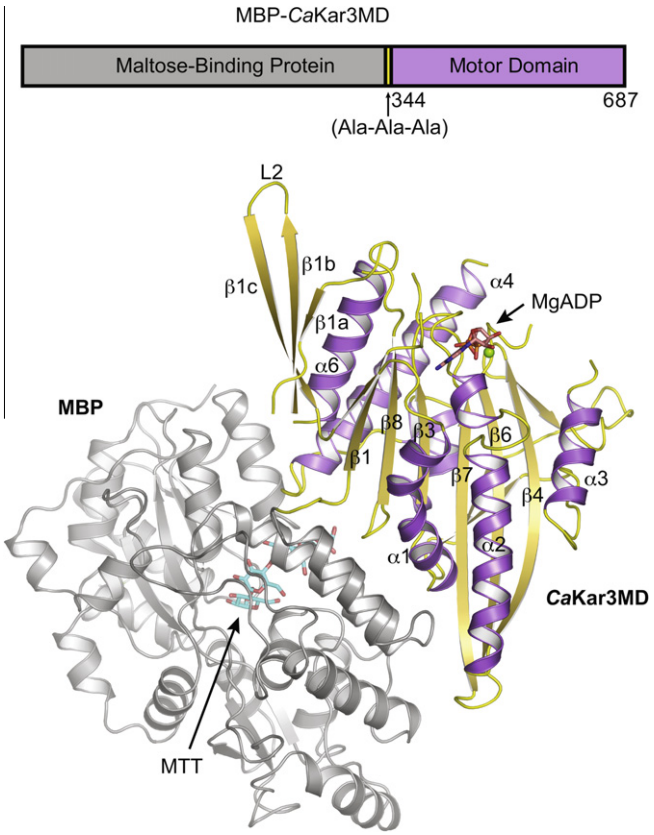


**Fig. 2.** The structure of MBP–*Ca*Kar3MD. (A) Schematic drawing of the MBP–*Ca*Kar3MD construct, indicating the polyalanine linker sequence and the boundaries of the *Ca*Kar3 protein. (B) Ribbon representation of the structure of the motor domain of *Ca*Kar3 (in purple and orange) fused to MBP (in gray). This figure was created with PyMOL [48]. (For interpretation of the references to color in this figure legend, the reader is referred to the web version of this article.)

respectively. In all these structures, the Switch I element, which includes helix α3, loop L9, and helix α3a, is partially unstructured and the portions of α3 that could be modeled in each structure are angled away from the active site. Together with Switch II (loop L11, helix α4, loop L12, helix α5 and loop L13), this region helps organize catalytic water molecules and forms a nucleotide γ-phosphate sensing mechanism in the nucleotide-binding pocket of kinesins, myosins, and G-proteins [35,36].

A unique structural feature of *Ca*Kar3 involves the exposed L1 loop in which the RxRP nucleotide base-binding motif resides (Fig. 1B). This structure forms the top edge of the nucleotide-binding pocket and exhibits some structural variability among kinesin family members [37]. In *Ca*Kar3, the RxRP motif is disrupted by substitution of asparagine for the proline residue, and by insertion of a long polyserine tract (aa 358–369), most of which is unstructured in the MBP–*Ca*Kar3MD molecule (Fig. 2B). Although polyserine sequences of this nature area common feature shared among yeast proteins [38], this structure appears to be unique to *C. albicans*. The functional implications of this difference are unknown. It could form a phosphorylation site that might be involved in regulating the ATPase activity of the enzyme, however, our observation of MgADP in the active site of MBP–*Ca*Kar3MD suggests that this is not a critical prerequisite for catalysis.

The divergences between *Ca*Kar3 and its homologs further extend to the electrostatic surface potential of the motor domain. A comparison of the solvent-accessible surfaces of the *Ca*Kar3 and *Sc*Kar3 motor domains reveals unique charge distribution along the α2 helix, and in loop L5, which divides this helix into helix α2a and α2b (Fig. 3). *Ca*Kar3 shows a preponderance of negative change toward the C-terminus of α2b (the lower part of the motor domain in the diagram), while *Sc*Kar3 is dominated by positively charged residues (lysines) in this region. The small β1-lobe at the edge of the motor domain is also much more highly populated with negatively charged amino acids than *Ca*Kar3. This indicates that, despite the extensive shared fold identity, each form of Kar3 kinesin is tailored for recognition by unique regulatory molecules or for different interactions with domains external to the motor core. Conversely, the rear surface of these proteins exhibits less obvious discrepancies in their electrostatic charge patterning, and are both mainly positively charged (not shown). This is the surface through which microtubule interactions occur [39,40].

### 3.3. Interactions between MBP and the CaKar3 motor domain

The MBP and *Ca*Kar3MD modules interact through several areas of shape and chemical complementarity, burying ~880 Å$^2$ of sol-

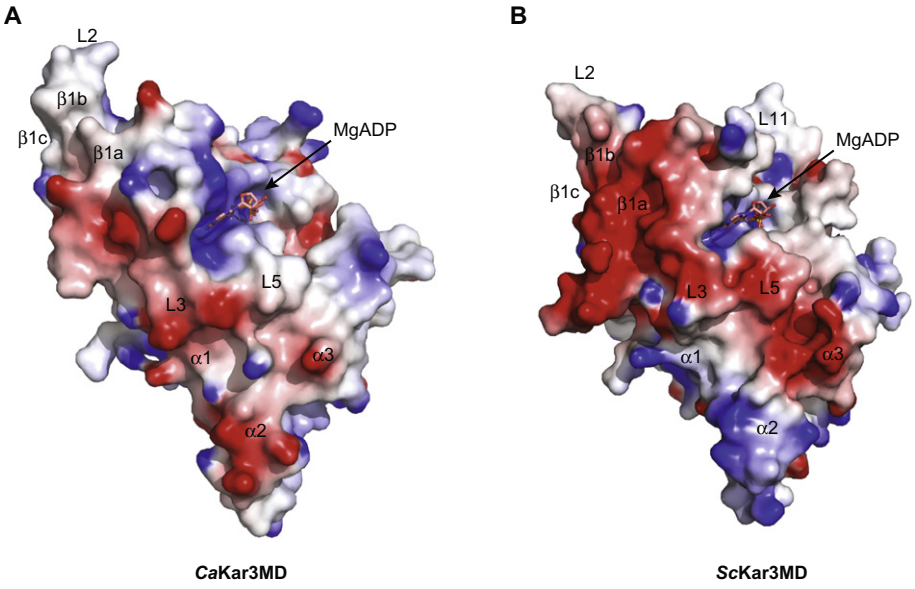


**Fig. 3.** Comparison of the electrostatic surfaces of *Ca*Kar3MD and *Sc*Kar3MD. Electrostatic surface potential for the motor domains of (A) CaKar3 and (B) *Sc*Kar3 (PDB: 4ETP) were calculated using the Poisson–Boltzman solver Delphi [49] and the figures rendered in PyMOL.

vent accessible surface area on Kar3. Residues involved in this interface are found on loops L3, L6, L8b, L10, L12, and L13, and on the edge of strand β7 in the *Ca*Kar3 motor domain. These regions are highlighted in Fig. 1 and include several residues that are conserved among the Kinesin-14 family. The complementary surface on MBP is formed by helices II, III, XIII and XIV (Fig. 4A), which also form a major part of the sugar-binding pocket of MBP. These interactions may be occluding one or more surfaces on *Ca*Kar3 that are inherently flexible or prone to aggregation in the absence of the N-terminally attached neck portion of the protein, or its binding partner *Ca*Cik1 (unpublished results). They could also reduce the conformational flexibility of the fusion structure and facilitate crystallization. This may partly explain why crystallization of the untagged versions of *Ca*Kar3 was unsuccessful.

Interestingly, the site of interaction with MBP is close to, but unique from, the site of Kar3 and Ncd neck docking, which has been captured in crystal structures of the *Sc*Kar3Vik1 complex and a number of Ncd homodimer structures (Fig. 4A)[10,41,42]. Instead, the MBP interface overlaps more prominently with the site of neck-linker docking in conventional kinesins (Fig. 4B) [43–45]. Moreover, superposition of the coordinates for the Kar3 subunits of MBP–*Ca*Kar3MD and *Sc*Kar3Vik1 shows that the arrangement of MBP relative to *Ca*Kar3MD is distinct from the position occupied by the Vik1 subunit in the *Sc*Kar3Vik1 heterodimer (Fig. 4C). Combined with the conservation of some of the residues involved, this raises the question of whether or not the surface occupied by MBP forms yet another docking position for either the neck or the partner subunit of Kinesin-14 motors. In this regard, perhaps the *Sc*Kar3Vik1 and Ncd structures do not capture the full spectrum of the arrangements of these elements during the motile cycle. Alternatively, this interface may simply be unique to *Ca*Kar3, and it may or may not provide a docking site for the neck or partner subunits of *Ca*Kar3. MT cosedimentation analysis of MBP–*Ca*Kar3MD demonstrated that MBP does not interfere appreciably with MT binding as MBP–*Ca*Kar3MD partitioned with MTs in a tubulin concentration-dependent manner similarly to the untagged *Ca*Kar3MD construct (Fig. 4D).

In summary, by fusing maltose binding protein to the neck of the *C. albicans* Kar3 motor domain, we dramatically improved recombinant protein expression levels, protein solubility, and were able to grow crystals quickly and under a variety of precipitant conditions. Through this strategy we present the first high-resolution information on a motor protein from *C. albicans* fungi and the

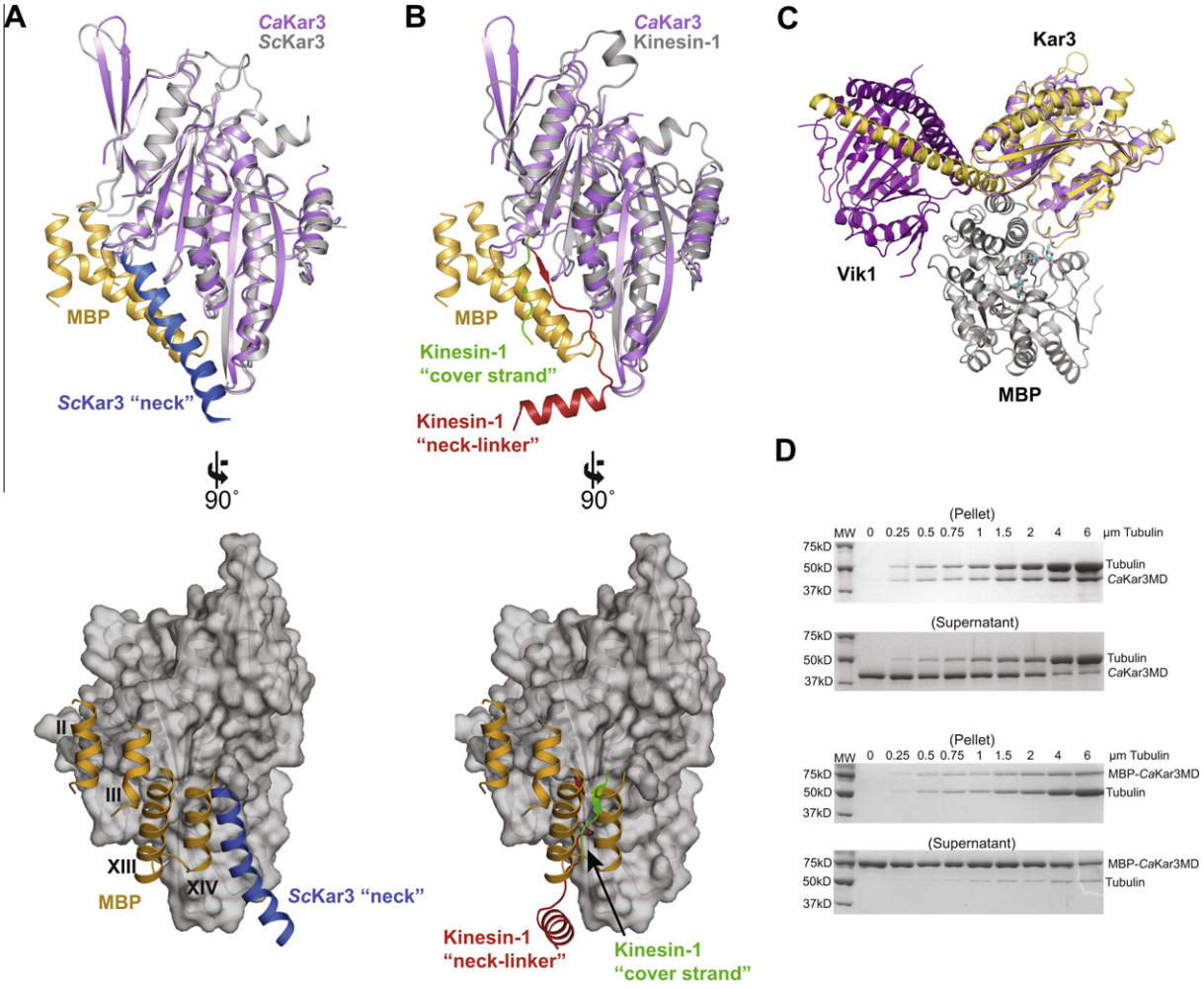


**Fig. 4.** Interactions between MBP and *Ca*Kar3MD. (A) Two views of *Ca*Kar3MD are shown superposed upon *Sc*Kar3 from the *Sc*Kar3Vik1 complex (PDB: 4ETP). The neck of *Sc*Kar3 is shown in blue. The helices contacting *Ca*Kar3 from MBP are shown in orange and are labeled according to the scheme of Spurlino et al. [50]. (B) Two views of *Ca*Kar3MD are shown superposed upon the rat Kinesin-1 structure (PDB: 2KIN), whose neck-linker cover strand are colored red and green, respectively. (C) MBP–*Ca*Kar3MD is shown superposed onto the structure of *Sc*Kar3Vik1 via alignment of the Cα atoms of their Kar3 motor domains. All molecules are colored separately and labeled in the figure. Maltotetraose is colored cyan. (D) Representative SDS–PAGE gels showing supernatant and pellet fractions of equilibrium microtubule co-sedimentation assays with *Ca*Kar3MD and MBP-*Ca*Kar3MD constructs (4 μM) in the presence of 2 mM MgAMPPNP and increasing tubulin concentrations. (For interpretation of the references to color in this figure legend, the reader is referred to the web version of this article.)

first structure of an MBP-kinesin chimera. From this structure, we observed extensive structural homology of *Ca*Kar3 with related kinesins, but found divergencies in the electrostatic topography of the motor domain and a unique polyserine insertion in one of the elements that composes that ATPase pocket. The close arrangement of the MBP and *Ca*Kar3 MD modules also highlights a surface on the *Ca*Kar3 motor core that may hold significance as a site of intramolecular or intermolecular interactions that are relevant to the function and/or regulation of this kinesin.

## Acknowledgments

We thank Fred Faucher and Da Duan for assistance with diffraction data collection and processing. This work was supported by funding to J.S.A. from Canadian Institutes of Health Research and the Ontario Early Researcher Award program. J.S.A holds a Canada Research Chair (Tier 2) in Structural Biology.

## References

[1] H. Miki, Y. Okada, N. Hirokawa, Analysis of the kinesin superfamily: insights into structure and function, Trends Cell Biol. 15 (2005) 467–476.
[2] L.S.B. Goldstein, With apologies to Scheherazade: tail of, 1001 kinesin motors, Ann. Rev. Genet. 27 (1993) 319–351.
[3] R.D. Vale, R.J. Fletterick, The design plan of kinesin motors, Ann. Rev. Cell Dev. Biol. 13 (1997) 745–777.
[4] C.J. Lawrence, R.K. Dawe, K.R. Christie, D.W. Cleveland, S.C. Dawson, S.A. Endow, L.S. Goldstein, H.V. Goodson, N. Hirokawa, J. Howard, R.L. Malmberg, J.R. McIntosh, H. Miki, T.J. Mitchison, Y. Okada, A.S. Reddy, W.M. Saxton, M. Schliwa, J.M. Scholey, R.D. Vale, C.E. Walczak, L. Wordeman, A standardized kinesin nomenclature, J. Cell Biol. 167 (2004) 19–22.
[5] N. Hirokawa, R. Takemura, Kinesin superfamily proteins and their various functions and dynamics, Exp. Cell Res. 301 (2004) 50–59.
[6] A.T. Mackey, L.R. Sproul, C.A. Sontag, L.L. Satterwhite, J.J. Correia, S.P. Gilbert, Mechanistic analysis of the Saccharomyces cerevisiae kinesin Kar3, J. Biol. Chem. 279 (2004) 51354–51361.
[7] P.B. Meluh, M.D. Rose, Kar3, a kinesin-related gene required for yeast nuclear fusion, Cell 60 (1990) 1029–1041.
[8] E.R. Hildebrandt, M.A. Hoyt, Mitotic motors in *Saccharomyces cerevisiae*, Biochim. Biophys. Acta 1496 (2000) 99–116.
[9] B.D. Page, L.L. Satterwhite, M.D. Rose, M. Snyder, Localization of the Kar3 kinesin heavy chain-related protein requires the Cik1 interacting protein, J. Cell Biol. 124 (1994) 507–519.
[10] K.C. Rank, C.J. Chen, J. Cope, K. Porche, A. Hoenger, S.P. Gilbert, I. Rayment, Kar3Vik1, a member of the Kinesin-14 superfamily, shows a novel kinesin microtubule binding pattern, J. Cell Biol. 197 (2012) 957–970.
[11] B.D. Manning, J.G. Barrett, J.A. Wallace, H. Granok, M. Snyder, Differential regulation of the Kar3p kinesin-related protein by two associated proteins, Cik1p and Vik1p, J. Cell Biol. 144 (1999) 1219–1233.
[12] M.K. Gardner, J. Haase, K. Mythreye, J.N. Molk, M. Anderson, A.P. Joglekar, E.T. O'Toole, M. Winey, E.D. Salmon, D.J. Odde, K. Bloom, The microtubule-based motor Kar3 and plus end-binding protein Bim1 provide structural support for the anaphase spindle, J. Cell Biol. 180 (2008) 91–100.
[13] B.D. Page, M. Snyder, Cik1: a developmentally regulated spindle pole body-associated protein important for microtubule functions in *Saccharomyces cerevisiae*, Genes Dev. 6 (1992) 1414–1429.
[14] J.G. Barrett, B.D. Manning, M. Snyder, The Kar3p kinesin-related protein forms a novel heterodimeric structure with its associated protein Cik1p, Mol. Biol. Cell 11 (2000) 2373–2385.
[15] B.D. Manning, M. Snyder, Drivers and passengers wanted! the role of kinesin-associated proteins, Trends Cell Biol. 10 (2000) 281–289.
[16] W. Saunders, V. Lengyel, M.A. Hoyt, Mitotic spindle function in Saccharomyces cerevisiae requires a balance between different types of kinesin-related motors, Mol. Biol. Cell 8 (1997) 1025–1033.
[17] W.S. Saunders, M.A. Hoyt, Kinesin-related proteins required for structural integrity of the mitotic spindle, Cell 70 (1992) 451–458.
[18] R.K. Sherwood, R.J. Bennett, Microtubule motor protein Kar3 is required for normal mitotic division and morphogenesis in *Candida albicans*, Eukaryot. Cell 7 (2008) 1460–1474.
[19] P.E. Sudbery, Growth of *Candida albicans* hyphae, Nat. Rev. Microbiol. 9 (2011) 737–748.
[20] F.C. Odds, *Candida* infections: an overview, Crit. Rev. Microbiol. 15 (1987) 1–5.
[21] A.M. Gulick, H. Song, S.A. Endow, I. Rayment, X-ray crystal structure of the yeast Kar3 motor domain complexed with Mg.ADP to 2.3 A resolution, Biochemistry 37 (1998) 1769–1776.
[22] M. Yun, X. Zhang, C.G. Park, H.W. Park, S.A. Endow, A structural pathway for activation of the kinesin motor ATPase, EMBO J. 20 (2001) 2611–2618.
[23] D. Duan, D.J. Hnatchuk, J. Brenner, D. Davis, J.S. Allingham, Crystal structure of the Kar3-like kinesin motor domain from the filamentous fungus *Ashbya gossypii*, Proteins 80 (2012) 1016–1027.
[24] A. Ke, C. Wolberger, Insights into binding cooperativity of MATa1/MATalpha2 from the crystal structure of a MATa1 homeodomain-maltose binding protein chimera, Protein Sci. 12 (2003) 306–312.
[25] L.R. Sproul, D.J. Anderson, A.T. Mackey, W.S. Saunders, S.P. Gilbert, Cik1 targets the minus-end kinesin depolymerase Kar3 to microtubule plus ends, Curr. Biol. 15 (2005) 1420–1427.
[26] W. Kabsch, XDS, Acta Crystallogr. D Biol. Crystallogr. 66 (2010) 125–132.
[27] A.J. McCoy, R.W. Grosse-Kunstleve, P.D. Adams, M.D. Winn, L.C. Storoni, R.J. Read, Phaser crystallographic software, J. Appl. Crystallogr. 40 (2007) 658–674.
[28] G.N. Murshudov, A.A. Vagin, E.J. Dodson, Refinement of macromolecular structures by the maximum-likelihood method, Acta Crystallogr. D Biol. Crystallogr. 53 (1997) 240–255.
[29] P. Emsley, K. Cowtan, Coot: model-building tools for molecular graphics, Acta Crystallogr. D Biol. Crystallogr. 60 (2004) 2126–2132.
[30] P.D. Adams, P.V. Afonine, G. Bunkoczi, V.B. Chen, I.W. Davis, N. Echols, J.J. Headd, L.W. Hung, G.J. Kapral, R.W. Grosse-Kunstleve, A.J. McCoy, N.W. Moriarty, R. Oeffner, R.J. Read, D.C. Richardson, J.S. Richardson, T.C. Terwilliger, P.H. Zwart, PHENIX: a comprehensive Python-based system for macromolecular structure solution, Acta Crystallogr. D Biol. Crystallogr. 66 (2010) 213–221.
[31] J.S. Allingham, L.R. Sproul, I. Rayment, S.P. Gilbert, Vik1 modulates microtubule–Kar3 interactions through a motor domain that lacks an active site, Cell 128 (2007) 1161–1172.
[32] E.P. Sablin, F.J. Kull, R. Cooke, R.D. Vale, R.J. Fletterick, Crystal structure of the motor domain of the kinesin-related motor Ncd, Nature 380 (1996) 555–559.
[33] M.K. Kim, Y.M. Lee, W. Kim, W. Choi, Complete sequence of a gene encoding KAR3-related kinesin-like protein in *Candida albicans*, J. Microbiol. 43 (2005) 406–410.
[34] F.J. Kull, E.P. Sablin, R. Lau, R.J. Fletterick, R.D. Vale, Crystal structure of the kinesin motor domain reveals a structural similarity to myosin, Nature 380 (1996) 550–555.
[35] R.D. Vale, Switches, latches, and amplifiers: common themes of G proteins and molecular motors, J. Cell Biol. 135 (1996) 291–302.
[36] F.J. Kull, S.A. Endow, Kinesin: switch I & II and the motor mechanism, J. Cell Sci. 115 (2002) 15–23.
[37] S. Sack, F.J. Kull, E. Mandelkow, Motor proteins of the kinesin family. Structures, variations, and nucleotide binding sites, Eur. J. Biochem. 262 (1999) 1–11.
[38] M. Huntley, G.B. Golding, Evolution of simple sequence in proteins, J. Mol. Evol. 51 (2000) 131–140.
[39] K. Hirose, J. Lowe, M. Alonso, R.A. Cross, L.A. Amos, Congruent docking of dimeric kinesin and Ncd into three-dimensional electron cryomicroscopy maps of microtubule–motor ADP complexes, Mol. Biol. Cell 10 (1999) 2063–2074.
[40] S. Lakamper, E. Meyhofer, The E-hook of tubulin interacts with kinesin's head to increase processivity and speed, Biophys. J. 89 (2005) 3223–3234.
[41] F. Kozielski, S. De Bonis, W.P. Burmeister, C. Cohen-Addad, R.H. Wade, The crystal structure of the minus-end-directed microtubule motor protein Ncd reveals variable dimer conformations, Structure 7 (1999) 1407–1416.
[42] M. Yun, C.E. Bronner, C.G. Park, S.S. Cha, H.W. Park, S.A. Endow, Rotation of the stalk/neck and one head in a new crystal structure of the kinesin motor protein, Ncd, EMBO J. 22 (2003) 5382–5389.
[43] S. Sack, J. Muller, A. Marx, M. Thormahlen, E.M. Mandelkow, S.T. Brady, E. Mandelkow, X-ray structure of motor and neck domains from rat brain kinesin, Biochemistry 36 (1997) 16155–16165.
[44] C.V. Sindelar, M.J. Budny, S. Rice, N. Naber, R. Fletterick, R. Cooke, Two conformations in the human kinesin power stroke defined by X-ray crystallography and EPR spectroscopy, Nat. Struct. Biol. 9 (2002) 844–848.
[45] F. Kozielski, S. Sack, A. Marx, M. Thormahlen, E. Schonbrunn, V. Biou, A. Thompson, E.M. Mandelkow, E. Mandelkow, The crystal structure of dimeric kinesin and implications for microtubule-dependent motility, Cell 91 (1997) 985–994.
[46] M.A. Larkin, G. Blackshields, N.P. Brown, R. Chenna, P.A. McGettigan, H. McWilliam, F. Valentin, I.M. Wallace, A. Wilm, R. Lopez, J.D. Thompson, T.J. Gibson, D.G. Higgins, Clustal W and Clustal X version 2.0, Bioinformatics 23 (2007) 2947–2948.
[47] A.M. Waterhouse, J.B. Procter, D.M. Martin, M. Clamp, G.J. Barton, Jalview version 2—a multiple sequence alignment editor and analysis workbench, Bioinformatics 25 (2009) 1189–1191.
[48] W.L. DeLano, The PyMOL Molecular Graphics System, DeLano Scientific LLC, San Carlos, CA, 2002.
[49] W. Rocchia, S. Sridharan, A. Nicholls, E. Alexov, A. Chiabrera, B. Honig, Rapid grid-based construction of the molecular surface and the use of induced surface charge to calculate reaction field energies: applications to the molecular systems and geometric objects, J. Comput. Chem. 23 (2002) 128–137.
[50] J.C. Spurlino, G.Y. Lu, F.A. Quiocho, The 2.3—a resolution structure of the maltose- or maltodextrin-binding protein, a primary receptor of bacterial active transport and chemotaxis, J. Biol. Chem. 266 (1991) 5202–5219.